Science of the Total Environment 644 (2018) 1399–1408

Contents lists available at ScienceDirect

Science of the Total Environment

journal homepage: www.elsevier.com/locate/scitotenv

Vegetation and terrain drivers of infiltration depth along a semiarid hillslope

M.J. Rossi [a,b,c,*], J.O. Ares [b], E.G. Jobbágy [d], E.R. Vivoni [e,f], R.W. Vervoort [c], A.P. Schreiner-McGraw [e], P.M. Saco [a]

[a] Faculty of Engineering and Built Environment, University of Newcastle, Callaghan, New South Wales, Australia
[b] Instituto para el Estudio de los Ecosistemas Continentales (IPEEC-CONICET), Puerto Madryn, Argentina
[c] School of Life and Environmental Sciences, The University of Sydney, Sydney, Australia
[d] Grupo de Estudios Ambientales, IMASL, Universidad Nacional de San Luis & CONICET, San Luis, Argentina
[e] School of Earth and Space Exploration, Arizona State University, Tempe, AZ 85287, USA
[f] School of Sustainable Engineering and the Built Environment, Arizona State University, Tempe, AZ 85287, USA

HIGHLIGHTS

- Vegetation and terrain affect spatial variation in shallow infiltration depth.
- Measurement of wetting front depths at various locations within vegetation patches
- Infiltration depths are variable within the vegetation patches.
- Infiltration variability is controlled by patch orientation, shape and terrain.
- Patch orientation dictates patch shape and distance to hillslope crest effect.

GRAPHICAL ABSTRACT

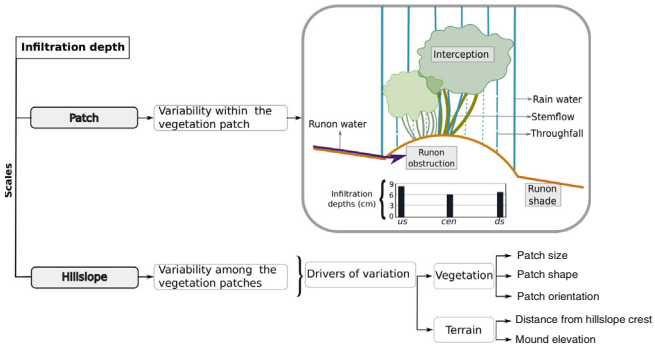

ARTICLE INFO

Article history:
Received 21 February 2018
Received in revised form 3 July 2018
Accepted 4 July 2018
Available online 23 July 2018

Editor: G. Ashantha Goonetilleke

Keywords:
Vegetation patch
Infiltration
Patch orientation
Patch shape
Patch size

ABSTRACT

An improved understanding of the drivers controlling infiltration patterns in semiarid regions is of key importance, as they have important implications for ecosystem productivity, retention of resources and the restoration of degraded areas. The infiltration depth variability (ΔInf) in vegetation patches at the hillslope scale can be driven by different factors along the hillslope. Here we investigate the effects of vegetation and terrain attributes under hypothesis that these attributes exert a major control in ΔInf within the patches. We characterise the ΔInf within vegetation patches at a semiarid hillslope located at the Jornada Experimental Range at dry antecedent conditions preceding two winter frontal rainfall events. We measured these events that are typical during winter conditions, and are characterised by low intensity (0.67 and 4.48 mm h^{-1}) and a total rainfall of 10.4 and 4.6 mm. High precision geo-referenced wetting front depth measurements were taken at various locations within the vegetation patches using differential GPS. Vegetation and terrain attributes were analysed to explain the ΔInf among the vegetation patches. The infiltration depths in the periphery of the patches were in general considerably deeper than those in the centre. The observations suggest that the upslope margin of the patches received additional water in the form of runon from upslope adjacent bare soil. Patch orientation with regard to the slope dictated the effect of the rest of the patch attributes and the distance to the hillslope crest on ΔInf. We found that primarily patch orientation, followed by shape and size modulate lateral surface water transport

* Corresponding author at: School of Engineering, Faculty of Engineering and Built Environment, University of Newcastle, University Drive, Callaghan, NSW 2308, Australia.
E-mail address: julieta.rossi@newcastle.edu.au (M.J. Rossi).

https://doi.org/10.1016/j.scitotenv.2018.07.052

through their effects on overland flow paths and water retention; something that would be obscured under more simplistic characterisations based on bare versus uniform vegetated soil discrimination.

Index of terms

Acronyms

BS	bare soil
cen	centre of the vegetation patch
ds	downslope margin of the vegetation patch
S1	Storm 1
S2	Storm 2
us	upslope margin of the vegetation patch
VS	vegetated soil

Variables

ΔInf	infiltration depth variability, cm
A	patch area, m^2
AR_{LW}	geometric aspect ratio of a vegetation patch, cm
C	patch compactness
D	distance from hillslope crest, m
Inf	infiltration depth, cm
Inf_{ds}	*Inf* measured in the downslope margin of the vegetated patch, cm
Inf_P	*Inf* per unit of rainfall, cm mm^{-1}
Inf_{us}	*Inf* measured in the upslope margin of the vegetated patch, cm
L	patch length, m
P	total precipitation at the end of the corresponding storm, mm
Per	patch perimeter, m
W	patch width, m

1. Introduction

A strong interrelation between vegetation and hydrology has been widely described in semiarid shrublands (Tongway et al., 2001; Puigdefábregas, 2005; Pan et al., 2017; Geris et al., 2017). Semiarid vegetation patterns are typically patchy and often characterised as a two-phase mosaic composed of vegetated soil (*VS*) patches and bare soil (*BS*) inter-patch areas (Aguiar and Sala, 1999; Ludwig et al., 2005) that differ in scale and shape (Rietkerk et al., 2002) and distribute water resources heterogeneously (Cammeraat and Imeson, 1999; Cerdà, 1997; Merino-Martín et al., 2011). Vegetation patches in such areas are known as "oases or fertile patches", and are maintained by the concentration of water and nutrients during water flows (Anderson and Hodgkinson, 1997; Okin et al., 2015). Semiarid shrubland patches are often characterised by the presence of micro-relief in the form of mounds (Rostagno and del Valle, 1988; Wu et al., 2016; Rossi and Ares, 2017). These ecosystems behave as a mosaic of source and sink areas for water redistribution, in which the *BS* inter-patch is the source area for runoff production and the vegetation patch functions as a sink for runon (Anderson and Hodgkinson, 1997; Lavee et al., 1998; Calvo-cases et al., 2003; Merino-Martín et al., 2011). Common spatial structures include patches orientated across the slope or banded vegetation patterns (Valentin et al., 1999; Tongway et al., 2001; Saco et al., 2007; Deblauwe et al., 2012) and other regular and irregular patterns such as spots, gaps and stripes (Couteron and Lejeune, 2001; Rietkerk et al., 2002; Barbier et al., 2006; Saco and Moreno-de Las Heras, 2013).

Shallow soil moisture distribution is critically important as most rainfall events are small and the infiltration or wetting front only reaches the top few centimeters of the soil (Newman et al., 1997; Cavanaugh et al., 2011; Ferrante et al., 2014; Traff et al., 2014). The shallow soil moisture distribution is influenced by the soil infiltration rates, which are modulated by vegetation. Although the vegetated patches may have large infiltration rates, the apparent or effective infiltration rate may be lower than the potential rate, and affected by the specific location of the patch (Thompson et al., 2011; Rossi and Ares, 2016), which affects the amount of water that reaches each location. Therefore, the amount of water that reaches specific locations of the vegetation patch, and ultimately affects the effective infiltration, depends on the water redistribution processes between vegetation patches and bare soil inter-patches.

An improved understanding of water redistribution processes in semiarid shrublands is crucial to properly manage (Moreno-de Las Heras et al., 2012; Paschalis et al., 2016) and restore (Fuentes et al., 2016) these complex patchy landscapes. Therefore, understanding the drivers of variation of shallow soil moisture in semiarid regions has direct implications for the management of ecosystem productivity (Yu et al., 2008), retention of resources (Wu et al., 2016) and the restoration of degraded areas (Fuentes et al., 2016). While there have been many studies on soil infiltration in semiarid areas, there is limited understanding of how the spatial arrangement of vegetation patches and inter-patches affect the spatial patterns of shallow soil moisture (Chen et al., 2013; Hao et al., 2016). However, the effect of vegetation patches on ecohydrological processes at the patch scale has received some attention (Magliano et al., 2015; Rossi and Ares, 2016), but there have been fewer attempts to describe the factors controlling infiltration variability at larger scales.

Moreover, most of the previous research on the functioning of patchy vegetation focusing on runoff and infiltration processes, has been conducted in banded vegetation. Knowledge is rather scarce on the ecohydrological interactions in patchy, non-banded vegetation, which is often structured in a spotted, striped or along-slope patch configurations (Wilcox et al., 2003; Ludwig et al., 2005). In this context our results for along-slope patches expand knowledge in this area.

The variability of shallow soil moisture can be analysed at several spatial scales. At the patch scale, there have been studies (Puigdefábregas et al., 1999; Katra et al., 2007; Merino-Martín et al., 2015) that analysed the redistribution of shallow soil moisture focusing on the physical attributes of the vegetation patches. This redistribution process ultimately affects the spatial distribution of shallow soil moisture within each individual patch. Terrain or slope attributes also affect shallow soil moisture in each individual patch by directing more or less runoff-runon that is intercepted within the patches. This variability of shallow soil moisture can be explained at the hillslope scale by quantifying the variables (vegetation and/or terrain) that affect these variations among all the patches of the hillslope. To our knowledge, there have been no attempts to quantify the variation of shallow soil moisture within the patches considering simultaneous influences of patch size, shape, orientation and terrain attributes.

In order to improve this understanding, an experimental study was conducted to quantify the variability of shallow soil infiltration depths (as an indicator of shallow soil moisture) within the vegetation patches

(patch scale), and to identify the factors controlling this variability among the patches at the hillslope scale. Two hypotheses regarding shallow infiltration in a semiarid shrubland were tested: - H1. At the patch scale, the infiltration depth pattern within the vegetation patch is not uniform; - H2. At the hillslope scale, the variability in the infiltration depth among the patches contains systematic components related to vegetation patch and terrain attributes.

2. Material and methods

The study was carried out on a north-facing hillslope (slope angle = 7.3%) in the Jornada Experimental Range located in the northern Chihuahuan Desert (NM, USA) (Fig. 1). As shown in the sub-decimeter imagery acquired with an unmanned aircraft by Laliberte and Rango (2011) (Fig. 1b), the hill-bottom is characterised by a higher abundance of herbaceous and smaller plant clusters, compared to the hill-top. Larger slope and fluvial erosion in the downslope area give rise to flow concentration as evidenced by the presence of rills or drainage lines. Vegetation patches inside these drainage lines were excluded from our analysis because a visual analysis confirmed that the soil in these areas has a very high gravel content, and because these patches are dynamic due to the erosion processes and therefore cannot be interpreted in terms of a stable hillslope vegetation arrangement. 70% of the sampled patches at this mixed shrubland are orientated across the line of maximum slope and the other 30% are along the slope.

Soils at the site are primarily sandy loams with high gravel contents and a calcium carbonate layer present at approximately 40 cm depth (Anderson, 2013). A detailed soil texture analysis, performed by Anderson and Vivoni (2016) for the top 30 cm of soil, found that the soil is composed of 35% gravel, 32% sand, 28% silt, and 5% clay. Bare soil represents 66% of the total areal coverage of the site. The major vegetation types of the site are represented by shrubs (27%), grasses (6%) and cacti (1%). The mixed shrubland ecosystem at the site consists of creosote bush (*Larrea tridentata*), honey mesquite (*Prosopis glandulosa* Torr.), several grass species (*Muhlenbergia porteri*, *Pleuraphis mutica*, and *Sporobolus cryptandrus*), and other shrubs (*Parthenium incanum*, *Flourensia cernua*, and *Gutierrezia sarothrae*) (Schreiner-McGraw et al., 2016).

Precipitation at the site varies considerably over the year, with 53% of the long-term mean (245 mm yr^{-1}) occurring during the summer monsoon (Templeton et al., 2014). Thunderstorms in this region are the primary runoff generators and are typically of short duration (1 −2 h), high intensity (up to 250 mm h^{-1} for 5 min is common), and occur over limited areas (Renard, 1988).

A total of 52 random vegetation patches have been sampled at the north-facing hillslope (Fig. 1b) after two natural rainfall events (Supplementary Table 1) in October 2015 (4th and 19th). High precision georeferenced wetting front depth measurements were taken at the vegetation patches by means of a differential GPS (Trimble GPS GeoExplorer 6000), ensuring a very high precision in measurements (i.e. centimeters). Additionally, differential corrections were done on the points after collection.

The first storm (S1) lasted 15 h, and the second (S2) lasted 1 h. However, both storms are typical winter frontal storms with low intensity rainfall (0.67 and 4.48 mm h^{-1}) that generally results in little runoff. Antecedent soil moisture conditions 2 h prior both storms were similar (0.053 and 0.015 m^3 m^{-3}, Supplementary Table 1), as indicated by readings of soil dielectric sensors (Hydra Probe, StevensWater) situated at the north-facing hillslope.

The wetting front depths (infiltration depths) were identified as in Bhark and Small (2003) by digging and visualising the strong colour contrast between wet and dry soil. Given that this was destructive sampling, the samples were taken at different patches for each storm. The digging work was completed in less than 6 h after each storm event. At this time the drying front was a thin dry layer of superficial soil (less than 1 cm), and the wetting front remained unaffected.

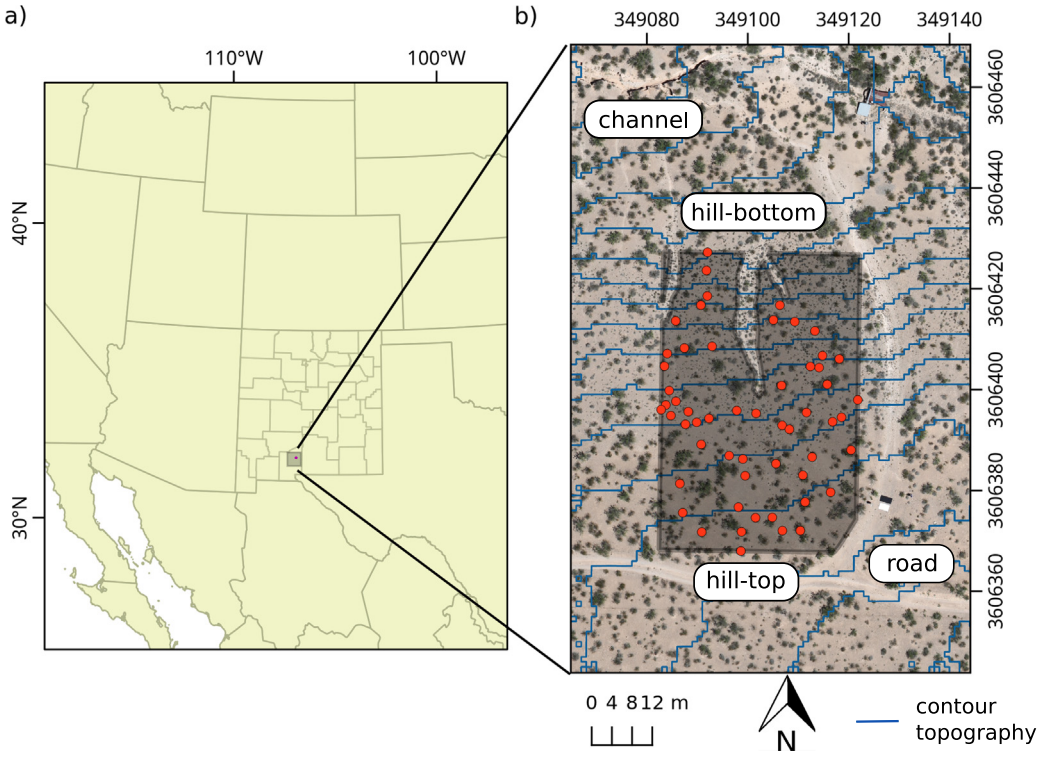

Fig. 1. a) Location of the field site (New Mexico State, USA). b) Sub-decimeter imagery of the hillslope studied overlaid to the contour topography (blue) lines (50 cm interval). The location of the sampled area and vegetation patches are indicated by the shaded area and red dots, respectively.

The rainfall observations were recorded using four tipping-bucket rain gauges (TE525MM, Texas Electronics) to construct a 30 min resolution spatial average based on Thiessen polygons (Schreiner-McGraw et al., 2016). At the hillslope scale of our measurements, it is safe to assume that the rainfall input is spatially uniform. The study area is too small to consider rainfall spatial heterogeneities and the difference in elevation is too low to affect rainfall patterns in any significant way. Additionally, the differences in rainfall among the four tipping-bucket rain gauges are very small due to their close proximity.

The water table at the study site is 90–105 m below the surface (King and Hawley, 1975), so it did not affect our infiltration measurements. Moreover, during low intensity winter precipitation, percolation occurs at much longer timescales of several days (Templeton et al., 2014; Pierini et al., 2014), and as our infiltration measurements were recorded between 2 and 14 h after the storms, we assume that leakage was negligible during the experiment. Our assumption is also supported by other studies conducted at our study site that found that the percolation beyond a depth of 40 cm is infrequent even during the larger summer monsoon storms (Schreiner-McGraw et al., 2016); and that no diffuse recharge is provided by the hillslopes (Schreiner-McGraw and Vivoni, 2017).

Infiltration depth (*Inf*, cm) was measured (2 h after storm 1 and 14 h after storm 2, which ended at 5 pm) at the following locations:

1. Within each vegetation patch or vegetated soil (*VS*): at the upslope margin (*us*) and downslope margin (*ds*) of the patch.
2. Additional infiltration depths at the centre (*cen*) of the vegetation patch (near the plant stems) at nine vegetation patches.

Infiltration depth per unit of rainfall (cm mm^{-1}) was estimated as:

$$Inf_P = Inf/P \tag{1}$$

where P is the total precipitation at the end of the corresponding storm (mm).

Infiltration depth variability (ΔInf) within vegetation patches was calculated as the difference between *Inf* measured in the upslope margin (Inf_{us}) and downslope margin (Inf_{ds}) of each patch:

$$\Delta Inf = Inf_{us} - Inf_{ds} \tag{2}$$

Vegetation and terrain attributes were analysed to explain the infiltration variability (Eq. (2)) among the vegetation patches at the hillslope scale. These attributes were derived from the sub-decimeter imagery acquired by Laliberte and Rango (2011), a 1 meter digital elevation model (DEM) derived from unmanned aerial vehicle images at a height of 200 m in October 2010 (Templeton et al., 2014) and 3D point coordinates recorded with a Trimble GPS GeoExplorer 6000.

The terrain attributes computed and analysed in this study include: distance from the hillslope crest (*D*, m) and upslope mound elevation (m). The distance from the hillslope crest was estimated for each vegetation patch and measured with respect to the upslope edge of the hillslope (Fig. 1). The upslope mound elevation (m) was calculated as the difference of altitude (recorded with the GPS) between the upslope margin of the vegetation patch and the near upslope bare soil interpatch.

The vegetation attributes computed and analysed in this study include: (i) patch size: area (*A*, m^2), perimeter (*Per*, m), length (*L*, m), width (*W*, m); (ii) patch shape: compactness (*C*) and geometric aspect ratio (AR_{LW}), and (iii) patch orientation with respect to the line of maximum slope. These attributes were estimated from the sub-decimeter imagery, the DEM and the GPS point coordinates.

The vegetation patch area and perimeter were estimated from the high resolution image. Length and width for each vegetation patch were computed as the longer and shorter sides of the patch (respectively).

The vegetation patch compactness, as an expression of patch arrangement in relation to space (a circle being the most compact shape), was calculated using the r.pi module of GRASS GIS (Wegmann et al., 2017) as:

$$C = \frac{Per}{2 * \sqrt{\pi * A}} \tag{3}$$

The geometric aspect ratio (AR_{LW}) of each vegetation patch was calculated as a patch elongation indicator, as the ratio of the longer side to the shorter side:

$$AR_{LW} = L/W \tag{4}$$

The orientation of the vegetation patch with respect to the line of maximum slope (across or along the slope) was estimated for each patch by calculating the azimuth of the longer side (patch length) of the vegetation patch. The azimuth was calculated as an angle between the North direction and the line of the patch length. The vegetation patches oriented NE (45° ± 22.5°), SW (225° ± 22.5°), E (90° ± 22.5°) and W (270° ± 22.5°) were classified as patches orientated across the line of maximum slope (across-slope). Whereas the patches oriented N (0° ± 22.5°), S (180° ± 22.5°), SE (135° ± 22.5°) and NW (315° ± 22.5°) were classified as patches orientated along the line of maximum slope (along-slope). The patches with geometric aspect ratio (Eq. (4)) values between 0.9 and 1.1 were classified as spotted, with no orientation.

Stepwise multiple linear regression was used to determine the variables (vegetation and terrain attributes) that could account for the maximum amount of variance of ΔInf (Eq. (2)) at the hillslope scale. The variable selection was performed using stepAIC function (Akaike Information Criterion) in the R library MASS (Venables and Ripley, 2002) using direction "backward". AIC selects the model that minimizes the expected, relative Kullback–Leibler information loss, and is useful in selecting the best model among all competing models (Akaike, 1974).

3. Results

3.1. Patch scale: infiltration depths within vegetation patches

It was found that water infiltration depth is not homogeneously distributed at the vegetation patch upslope and downslope margins, but varies according to the position with respect to the general terrain slope. The infiltration depth (*Inf*) measured upslope the vegetation patches was in all cases deeper or equal to the *Inf* measured downslope. Accordingly, the average *Inf* measured upslope (8.09 cm) was significantly (*t* value: −5.698; *P*: 1.313e−07; *n*: 109) deeper than the average *Inf* measured downslope (6.16 cm).

The Inf_P (infiltration depth per unit of rain) varied significantly (*t* value: −8.41; *P*: 5.642e−11; *n*: 61) between storm events. After the short storm (S2), the average infiltration per unit of rain (1.26 cm mm^{-1}) at the patches was deeper than average Inf_P (0.73 cm mm^{-1}) after the long storm (S1). The same Inf_P trend was observed for the upslope (*t* value: −10.31; *P*: 1.83e−09; *n*: 61) and downslope (*t* value: −6.14; *P*: 9.133e−06; *n*: 61) margins of the patches. Additionally, the upslope and downslope Inf_P differences were larger after the short storm (S2, $us - ds$: 0.43 cm mm^{-1}) as compared to the long storm (S1, $us - ds$: 0.17 cm mm^{-1}).

However, as S1 lasted longer (15 h) than S2 (1 h); the average final infiltration depth at the vegetation patches was significantly (*t* value: −4.94 *P*: 5.055e−6; *n*: 61) larger for S1 (7.62 cm) than that for S2 (5.84 cm) (Fig. 2).

In addition to the difference detected for infiltration at the upper and lower margins of the vegetation patches, infiltration also varied at the sampled centre position within the patch (Fig. 3). In the majority of the cases (six out of nine patches) in which we measured *Inf* in the

centre, the *Inf* was deeper at the periphery (Fig. 3a, c, d, f, g, i), that was defined as the average between upslope and downslope *Inf* margin measurements. Two out of nine patches had a deeper average *Inf* in the centre as compared to the periphery of the patch (Fig. 3e, h) and one patch had the same average *Inf* at the periphery and in the centre (Fig. 3b).

3.2. Hillslope scale: variation of infiltration depth among vegetation patches

The infiltration depth variability (ΔInf, Eq. (2)) among the vegetation patches at the hillslope scale is not only affected by the geometrical attributes of the vegetation patches themselves, but also by the terrain attributes that determine the amount of runoff that is intercepted and captured by the vegetation patches. The results presented below relate to both.

Although vegetation attributes were not significant in explaining the infiltration variability for the entire population of patches, they became significant when the patches were grouped into two categories according to their spatial orientation. Fig. 4 shows significant univariate regressions between ΔInf at the across-slope and along-slope vegetation patches and vegetation attributes. The regression slopes are positive or negative according to the patch orientation (across-slope and along-slope, respectively). However, all the along-slope univariate regressions loose statistical significance if an outlier is eliminated.

Results from the multiple linear regression analysis of the across-slope vegetation patches are indicated in Table 1, which indicates the independent variables which explain the variability in ΔInf among these patches. The distance from the hillslope crest (D, m) is related to increasing ΔInf at across-slope patches. Patch length is significantly related to increasing ΔInf in both the univariate and multivariate analysis. Increasing geometric aspect ratio of the vegetation patch (AR_{LW}) and mound elevation are both linked to decreasing ΔInf or a homogeneous water infiltration depth in the across-slope patches.

Table 2 displays the results from the multiple linear regression analysis for the along-slope vegetation patches, including both the main effects and an interaction term ($D \times$ patch compactness (C)). An interaction effect exists when the effect of the independent variable on the dependent variable differs depending on the value of a third variable, called the moderator. The significant variables at the 0.05 level which explain the variability of ΔInf among the along-slope vegetation patches, are indicated in Table 2. Increasing D and C are related to a decreasing ΔInf (0.13 and 1.9 cm, respectively), which means that the water infiltration depth is uniformly distributed inside these type of patches. The effect of D on ΔInf increases by 0.05 for every unit increase in C. This also works the other way around.

The regression coefficients for D and C reflect conditional relationships: −0.127 reflects the influence of D on ΔInf when C remains constant, and −1.890 reflects the influence of C on ΔInf when D remains constant. The coefficient 0.049 represents an interaction effect that estimates the change in the slope of ΔInf on D given a one unit change in the moderator C (or, alternatively, the change in the slope of ΔInf on C given a one unit change in the moderator D).

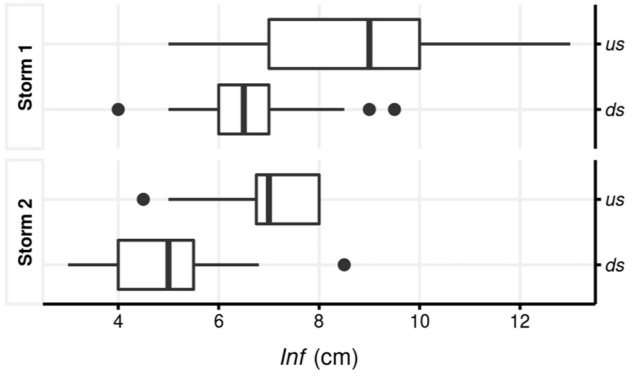

Fig. 2. Boxplots of water infiltration depth (*Inf*) measured upslope (*us*) and downslope (*ds*) margin of the vegetation patches according to the storm event (see Table 1). Bold line represents median, box the interquartile range, whiskers are 1.5× interquartile range from median, points outliers.

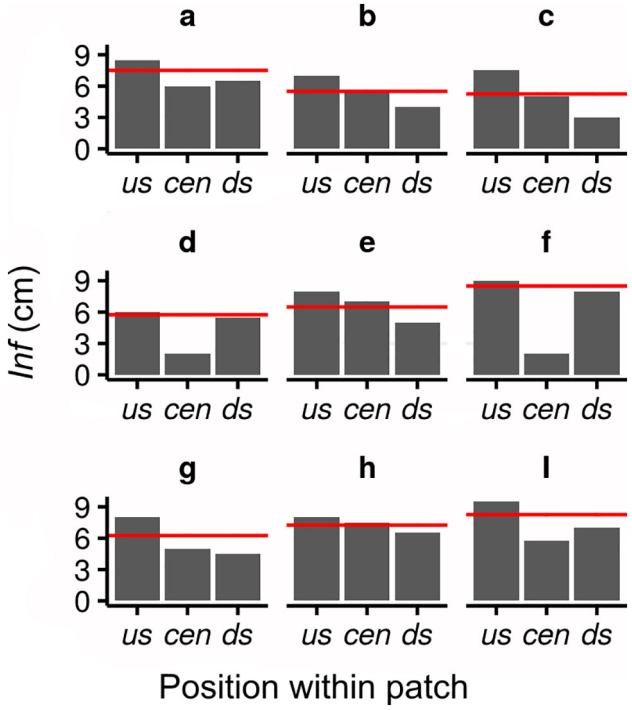

Fig. 3. Water infiltration depth (*Inf*) measured at the upslope (*us*) margin, downslope (*ds*) margin and centre (*cen*) of different vegetation patches. Red lines indicate the *Inf* at the periphery (calculated as the average *us* and *ds* measurements) of the vegetation patch.

The results of a Johnson and Neyman (1936) procedure shown in Fig. 5 can be used to assess the extent to which the effect that the predictor variables shown in Table 2 have on the ΔInf across different levels of their moderators. It can be observed that the conditional slope of the D (predictor shown at Fig. 5a) is significant when the C (moderator) is less than 2.11 and larger than 4. Also, the conditional slope of the C (predictor shown at Fig. 5b) is significantly different from zero (and in this case negative) when the D (moderator) is less than 27.8 m.

4. Discussion

The focus of this work is on the spatial variation of shallow soil infiltration depths (as an indicator of shallow soil moisture) that occur during two typical winter frontal low intensity rainfall events with dry antecedent conditions. Longer time scale processes that influence soil moisture distribution (evaporation, transpiration) were not examined.

4.1. Drivers of variation in infiltration depth within the vegetation patches

Inf (infiltration depths) within vegetation patches (Figs. 3 and 4) were shown to be variable in space. Moreover, the *Inf* pattern within the patches was not random, but in general the infiltration was deeper in the periphery of the vegetation patches as compared to the centre (Fig. 3). This points to the role of rainfall interception which is spatially variable within the area beneath herbaceous and/or woody vegetation canopies (Dunkerley, 2002; Lozano-Parra et al., 2015; Stoof et al., 2012; Magliano et al., 2015). It has been proved that dry antecedent conditions (as in this experimental study) can affect shrub interception by storing water that would be subsequently evaporated from the shrub

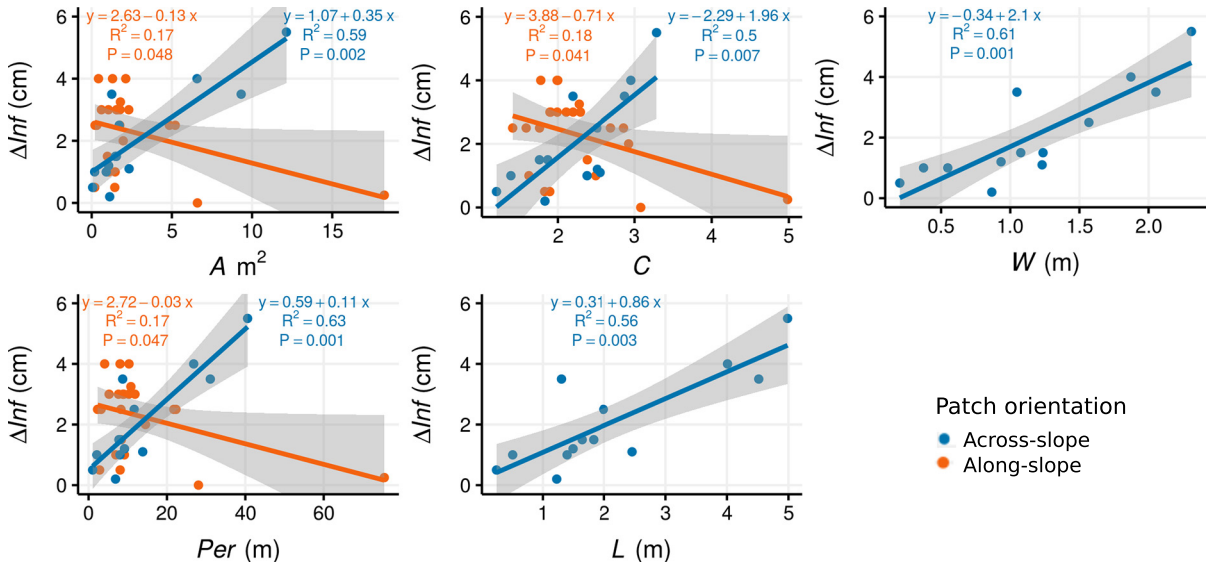

Fig. 4. Univariate regressions of infiltration depth variability (Δ*Inf*) among the vegetation patches and their attributes (area (*A*), perimeter (*Per*), length (*L*), compactness (*C*) and width (*W*)) at the across-slope and along-slope vegetation patches.

canopy (Magliano et al., 2015). Therefore, it is expected that *inf* measurements obtained in wetter conditions will be deeper than those from this study. In wetter antecedent conditions than those in this study, the infiltration in the centre of the vegetated patches may be greater than the measurements obtained here due to the effect of funneling flow that occurs on stems (Garcia-Estringana et al., 2010).

Even if the interception and hydraulic conductivity within the vegetation patch were uniform in space, the effective infiltration rate would be variable and dependent on the overland flow contribution, which varies as the upslope portions of the mound tend to receive more runon. This leads to faster and deeper water infiltration flow (preferential flow) than what would be expected by the classical flow theory. This latter effect has been shown to be particularly relevant in banded vegetation by differences in vegetation growth at the upslope and downslope patch margins (Berg and Dunkerley, 2004) and evidence of ponding processes at the upslope margin (Galle et al., 1999). Previous studies have shown that overland flow metrics (Marques et al., 2007; Rossi and Ares, 2016) and infiltration rates vary within the vegetation patches.

In addition, the hydraulic conductivity within a vegetation patch is generally not uniform in space. Dunkerley (2002) described the spatial pattern of infiltration rates in a mulga woodland in arid central Australia. In his work, infiltration rates measured with miniature cylinder infiltrometers were highest in close proximity to the plant stems, and declined rapidly with increasing distance. Here we analysed effective infiltration depths for actual rainfall events instead of potential infiltration rates. The difference between these measurements is that the centre of the patch may have a larger infiltration rate (due to enhanced vegetated soil (*VS*) physical properties) but the water (effective rainfall) that reaches that area is less than the total incoming water (effective rainfall + runon) that reaches the periphery of the patches. This may be attributed to rainfall interception (as explained previously) and/or to the topographic gradient at the mounds (terrain elevations on which the vegetation patches usually stand). Regarding the influence of the mounds on the infiltration depths, the periphery of the patches receives additional water in the form of runon from upslope adjacent bare soil (*BS*) inter-patches, whereas the centre of the patches may only receive water from stemflow and throughfall (Rossi and Ares, 2016) or receives less water than the patch periphery due to its higher topographical position.

These results are consistent with previous studies (Puigdefábregas and Sánchez, 1996; Puigdefábregas et al., 1999; Puigdefábregas, 2005) that found significant differences between water fluxes measured at varying positions in relation to tussocks stands, with approximately 50% of runoff produced in *BS* intercepted in the upper portion of the tussocks stands. This pattern of infiltration at the patch margins in which infiltration is higher in the upstream portions as compared to the downstream portions, is defined in this study as "runon shade", and occurs as follows: runoff is generated in the less permeable *BS* areas and flows downslope reaching the vegetation patch and associated mound. The latter, with a higher infiltration capacity, gain water produced by the upstream *BS* areas (Scoging et al., 1992; Galle et al., 1999). As a result, the upslope margin of the vegetated mound would tend to receive more water than the downslope margin, and higher (lower) infiltration (preferential flow) occurs in the upslope (downslope) margin. Moreover, numerical (Thompson et al., 2011; Rossi and Ares, 2017) and field based evidence (Rossi and Ares, 2016, 2017) indicate that the topographic gradient at the vegetation mound and their surface roughness could impede lateral redistribution from surrounding *BS*, or at least confine redistribution strongly to the edges of the vegetated mounds. This is reflected in the lower *Inf* values at the centre of the vegetation patches (a, c, d, f, g, i) shown in Fig. 3.

Table 1
Multiple linear regression of infiltration depth variability (Δ*Inf*) for the across-slope orientated vegetation patches ($R^2 = 0.78$, $P = 0.0104$).

	β coefficient Non standardized	*t* Value	*P*
Intercept	32.701	−2.28	0.0507
D	0.152	2.28	0.0520
AR_{LW}	−1.882	−2.05	0.0750
L	0.770	2.57	0.0332
Mound elevation	−0.415	−2.22	0.0571

Table 2
Multiple linear regression of variation in infiltration depth (Δ*Inf*) for the along-slope orientated vegetation patches ($R^2 = 0.47$, $P = 0.00375$).

	β coefficient Non standardized	*t* value	*P*
Intercept	7.115	5.78	9.7e-06
D	−0.127	−2.84	0.0098
C	−1.890	−3.89	0.0008
D:*C*	0.049	2.57	0.0178

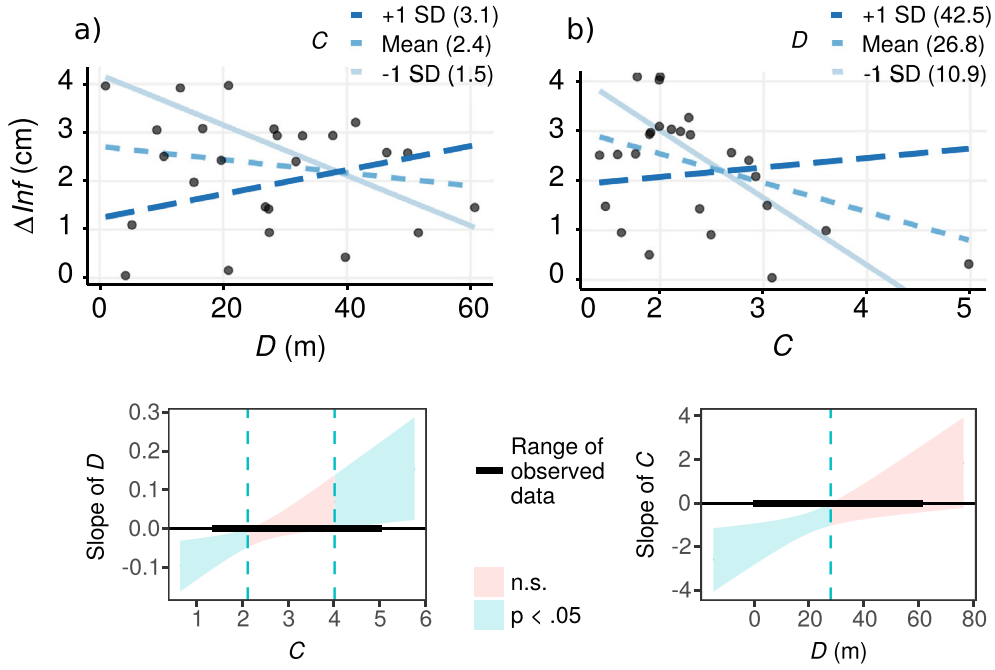

Fig. 5. (Above) Regressions of infiltration depth variability (Δ*Inf*) among the along-slope patches and a) distance from the hillslope crest (*D*) and b) vegetation patch compactness (*C*) according to their moderators. (Below) Johnson-Neyman intervals indicating the predictor's slope significance.

The average final *Inf* at the vegetation patches was deeper after S1 as compared to S2 (Fig. 2). This is to be expected as the short duration of the S2 reduced the opportunity for infiltration, and runon water that could have been infiltrated in the vegetation patches is lost as runoff. Although only two storms were sampled, these are representative for 2015 (average rainfall intensity: 1.3 mm h^{-1}) according to the instrument record at the study site. Moreover, we focus on the processes of infiltration and while other storms might give slightly different results, the pattern and influence of the processes is not likely to change.

In summary, the field evidence in this section did not detect uniform infiltration depth patterns within the vegetation patches and supports hypothesis 1. Fig. 6 aims to summarize this section by illustrating the infiltration depth patterns within vegetation patches and the mechanisms that are responsible for the observed variability.

4.2. Drivers of variation in infiltration depth among patches

Here we discuss the drivers of variation in Δ*Inf* among vegetation patches (hillslope scale) focusing first in the effects of vegetation attributes and later on the terrain attributes.

4.2.1. Effects of vegetation attributes

The results for shallow infiltration shown in Fig. 4 are in agreement with previous studies showing that the spatial patterns of shallow soil moisture within semiarid hillslopes are tightly related to the spatial patterns of vegetation cover (Bautista et al., 2007; Traff et al., 2014). In addition we find that vegetation patch orientation can modulate the variation in Δ*Inf*.

Vegetation patch size attributes (area, perimeter, length, and width) were found to be only significant in explaining the variation of infiltration of across-slope patches. The regression analysis indicates that across-slope larger patch size attributes relate to more variation in Δ*Inf* among the vegetation patches. This could be due to the presence of vegetation stems, litter and the effect of microtopography that increases the friction encountered by water flowing under the vegetation surface and the detention storage (Dunne et al., 1991; Jin et al., 2000; Howes and Abrahams, 2003; Marques et al., 2007; Mekonnen et al., 2016; Rossi and Ares, 2016). Galle et al. (1999) reported measuring low runoff in the upslope border of vegetated bands (reaching the body or centre) and attributed it to the presence of natural obstacles (roots, leaves) that create local zones where water is temporarily stored allowing longer time for surface storage infiltration. Therefore, larger

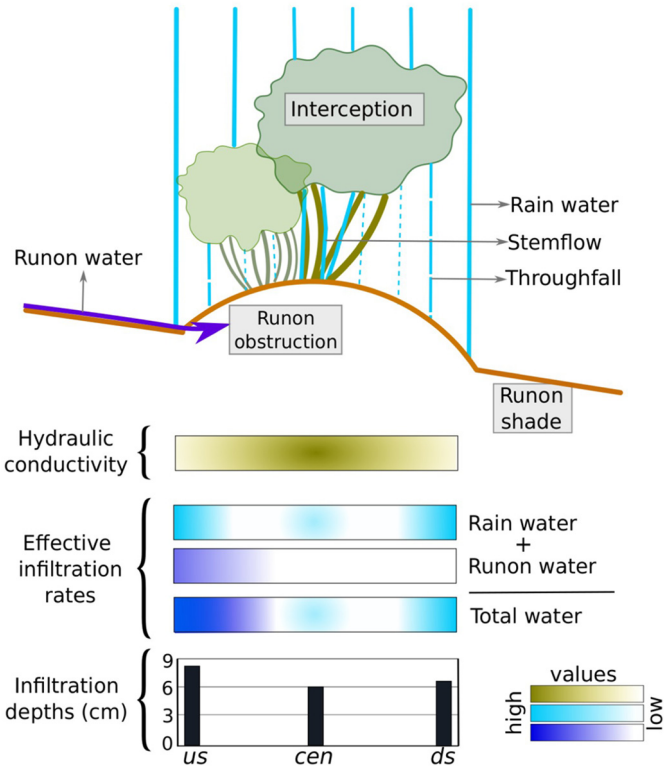

Fig. 6. Schematic summary of the infiltration depth pattern within the vegetation patches. Rain water is less intense within the patch as a consequence of interception. Runon water is less intense at the downslope margin of the patch as a consequence of runon obstruction and "runon shade" (also see Supplementary Fig. 2). Infiltration depth data corresponds to actual data of a vegetation patch shown in Fig. 3a.

patch size increases possible obstructions (friction) to the runon flow reaching the across-slope patch, increasing runon retention and infiltration at the upslope margin, and decreasing opportunities for runon infiltration at the downslope margin of the vegetation patch. This difference in infiltration rates at the patch margins generates a larger variation in infiltration depth.

In line with the above mentioned result, previous simulation modeling (Boer and Puigdefábregas, 2005) and field observations (Abrahams et al., 1995; Wainwright et al., 2000; Bautista et al., 2007) have shown that fine-grained (small patch size attributes) vegetation patterns are more efficient than coarse-grained (large patch size attributes) patterns in capturing water and sediment fluxes. The coarse-grained across-slope patches have larger upslope surface that retains (friction) and infiltrates more runon water at the upslope margin and therefore little or no runon is available for infiltration at the downslope margin, which is consequently only/mostly rainfed. These coarse-grained across-slope patches act as mulga bands of vegetation that have shown a similar infiltration trend at upslope and downslope areas (Tongway et al., 2001).

On the other hand, fine-grained across-slope vegetation patterns (as indicated by patch size attributes) have less ΔInf among the patches. These fine-grained patches have less upslope area to retain and infiltrate runon water, and therefore more runon is available for infiltration at the downslope margin. In addition to this friction effect that increases the retention (and infiltration) of water at the (larger or smaller) upslope area, shallow infiltration at the patches can also be increased by the effect of ponding that occurs at the upslope area. This will be discussed in Section 4.2.2.

Across-slope vegetation patch length is significantly related to increasing ΔInf at both univariate (Fig. 4) and multivariate (Table 1) analysis. As explained previously, larger patch size is associated with high values of surface roughness resulting from the presence of plant stems and their disturbing effect on the soil surface. Consequently, due to this flow resistance, more runon water would be obstructed at the upslope patch margin, decreasing the infiltration at the downslope margin, and increasing the infiltration depth variation at the vegetation patch.

The across-slope patch geometric aspect ratio (AR_{LW}, patch shape attribute) modulates the variation of infiltration similarly to the patch size attributes. As the across-slope ratio AR_{LW} increases (i.e. elongated patches), the water infiltration depth pattern becomes more uniform (Table 1). The elongated patch shape has larger relative upslope runon water accumulating zones (patch length) compared to the area through which the water has to flow through (patch width) to reach the downslope margin. This increased patch upslope area receives more runon water that flows through less resistance (friction) to reach the downslope margin (due to less relative patch width), leading therefore to more uniform water infiltration depth.

Regarding the patch compactness (Fig. 4), two across-slope patches with equal areas but different perimeters will have different compactness, with this measure being larger in the case of the patch with a larger perimeter. Therefore, as the across-slope patch compactness is lower, the spatial tortuosity in the patch becomes larger (more tortuous or twisted edges), increasing exposure to the runon water and leading to an accumulation of runon water at the tortuous upslope margin. This generates water accumulating zones that feed overland flow across the patch width, increasing the opportunity of the overland flow to reach and infiltrate the downslope margin of the vegetation patch (Supplementary Fig. 1).

A decrease in the along-slope patch's compactness (increase in its spatial tortuosity) is related to a larger ΔInf among the along-slope patches (Fig. 4 and Table 2). This case would retain and accumulate runon water at the along-slope patch tortuous upslope edges and probably retain it (Fig. 6). The mayor difference between the across-slope and along-slope cases is that in the first the water accumulated in the upslope margin flows through shorter paths (shorter than the patch's width) to reach the downslope margin; whereas in the latter case the runon water should flow across a larger area (patch's length) to reach the downslope margin, having more opportunity to be retained and infiltrate before reaching the downslope margin.

Moreover, as the patch distance from the hillslope crest increases (up to 27.8 m), the negative effect of the along-slope patch's compactness on ΔInf is increased by 0.05 m^{-1}. Therefore, a very tortuous along-slope patch would retain and infiltrate more water at the upslope margin if it is located near the middle of the hillslope (~28 m) rather than near the hillslope crest.

4.2.2. Effects of terrain attributes

In addition to the effects of the vegetation attributes, the variation in the infiltration depth among the patches is also related to the terrain attributes: distance from the hillslope crest (Tables 1 and 2) and mound elevation (Table 1). This is in agreement with well-known observations (in landscapes with banded/across-slope shrubs) showing that topography modulates the effect of vegetation on soil moisture patterns (Reid et al., 1999; Traff et al., 2014).

As the mound elevation of across-slope vegetation becomes greater, the runon water redistribution is strongly impeded to flow inside the vegetation patches due to their associated mound height, and the water infiltration depth pattern becomes more uniform (Table 1). As the mound elevation decreases, the overland flow is more likely to reach and infiltrate at the upslope margin of the patch, generating a strong contrast in infiltration between upslope and downslope portions of the vegetated mound. These results are consistent with numerical and field evidence (Thompson et al., 2011; Rossi and Ares, 2016, 2017) indicating that the vegetation mounds topographic gradient and surface roughness impede or constrain redistribution to their edges.

According to our results, an increase of 1 m from the hillslope crest is related to an increase of 0.15 cm depth in ΔInf at across-slope patches (Table 1). This means that the upslope patch margins receive more runon water than the downslope patch margins as the distance from the hillslope crest increases. As reported in many studies (Cerdan et al., 2004; Parsons et al., 2006; van de Giesen et al., 2000) runoff accumulation in the downslope direction may lead to an increase in runon available for infiltration. This generates deeper infiltration at the upslope margin which is likely to obstruct the runon, compared to the downslope margin of the across-slope patches.

However, this trend is not seen in the along-slope patches. Moreover, an increasing distance from the hillslope crest is related to a decreasing ΔInf (Table 2). This is probably associated to the fact that these patches are “thinner” than the across-slope patches in the direction of the line of maximum slope (or overland flow). This effect is increased by 0.05 m for every unit of patch compactness (or decrease in patch tortuosity) (Fig. 5a). Our results appear to be contradictory, as the distance from the hillslope crest that enhances overland flow has opposite effects on ΔInf at across-slope and (most) along-slope patches. This difference arises from the different orientation of the patches with respect to the line of maximum slope and the associated different runon path and runon shade generated by both patch orientations (Supplementary Fig. 2). It should be noted that the patches were not necessarily strictly orientated along/across the line of maximum slope, but their angles can range $\pm 22.5°$.

As explained previously, the presence of mounds associated with the vegetation patches can cause overland flow to diverge or run around them and as a result the water is not necessarily trapped in the centre and downslope of the shrub patches (Wilcox, 2003; Rossi and Ares, 2017). Therefore the orientation of the vegetation patch mound will determine the overland flow path. For instance, Supplementary Fig. 2 shows hypothetical cases with different patch (associated with a mound) orientations receiving runon water from the upslope bare soil. Runon water is impeded from flowing inside the patches due to the mound elevation, which diverges the surface flow. Runon water transits different paths depending on the orientation of the mound. It

is observed that the downslope patch margins of the across-slope oriented are less likely to receive and infiltrate runon than the downslope along-slope cases.

In relation to hypothesis H2, patch orientation was a key attribute in determining the effect of vegetation patch shape and terrain attributes in Δ*Inf* among the patches.

5. Conclusions

Based on two representative low intensity winter frontal storms and dry antecedent conditions, the infiltration depth spatial variability (Δ*Inf*) within the vegetation patches (patch scale) was controlled by vegetation and terrain attributes at the hillslope scale. We found that the spatial distribution of infiltration depths within the vegetation patches is not uniform. The Δ*Inf* at the hillslope scale is related to vegetation and terrain attributes, where the patch orientation with respect to the line of maximum slope is a key attribute that determines the effect on the infiltration depth pattern. For instance, the orientation of the vegetation patch (and its associated mound) will determine the overland flow path and water retention mechanism. This is particularly crucial in explaining how the distance from the hillslope crest, that enhances overland flow, generates opposite effects on Δ*Inf* at across-slope and along-slope patches.

Across-slope orientated patch size and compactness were significantly related to increasing infiltration variability. Therefore larger across-slope patch size and compactness would encourage the water and associated resources accumulation at the upslope margin. Additionally, patches orientated across-slope with small patch size attributes had less variation in Δ*Inf*, which reflected that the runon flowed flows through less resistance (friction) to reach the downslope margin (due to less relative patch width), leading therefore to a uniform water infiltration depth.

Through this study we found that the different shapes, sizes and orientations of vegetation patches determine water transfer mechanisms (overland flow paths and water retention mechanisms) that would be missed by a basic conceptualisation of bare versus uniform vegetated soil. While we have only sampled two low intensity winter frontal storms, our results and conclusions are fundamental to understand the dynamics of sites with similar physical and ecological characteristics. The key characteristics that give rise to the variability of infiltration rates that we found in our study are also present in many drylands worldwide. These correspond to ecological aspects such as effect of vegetation interception on rainfall and effects due to differences in vegetation growth at the upslope and downslope patch margins observed in banded vegetation. The key physical characteristics were found to be associated with changes in overland flow redistribution due to roughness of vegetation patches and the effect of overland flow divergence due to the topographic gradient at the vegetation mounds. Future work could further confirm or adjust this general model to different environmental conditions, by sampling other kinds of rainfall events and wetter antecedent conditions.

Acknowledgements

The corresponding author acknowledges the Consejo Nacional de Investigaciones Científicas y Técnicas (CONICET, Argentina) for a postdoctoral fellowship (003759/13). The Jornada Experimental Range is administered by the USDA-ARS and is a Long Term Ecological Research site funded by the National Science Foundation. We would like to acknowledge the New Mexico University (Sam Fernald) and USDA, Agricultural Research Service, Jornada Experimental Range (Albert Rango, John Anderson and Andrea Laliberte) for their logistical assistance and for providing imagery and topographical data. This work was partially supported by the ARC grant DP140104178. We thank anonymous reviewers for helpful comments that led to an overall improvement of the manuscript.

Appendix A. Supplementary data

Supplementary data to this article can be found online at https://doi.org/10.1016/j.scitotenv.2018.07.052.

References

Abrahams, A.D., Parsons, A.J., Wainwright, J., 1995. Effects of vegetation change on interrill runoff and erosion, Walnut Gulch, southern Arizona. Geomorphology 13, 37–48.
Aguiar, M.R., Sala, O.E., 1999. Patch structure, dynamics and implications for the functioning of arid ecosystems. Trends Ecol. Evol. 14 (7), 273–277.
Akaike, H., 1974. A new look at the statistical model identification. IEEE Trans. Autom. Control 19 (6), 716–723.
Anderson, C.A., 2013. Assessing Land-Atmosphere Interactions Through Distributed Footprint Sampling at Two Eddy Covariance Towers in Semiarid Ecosystems of the Southwestern U.S. (Masters of Science in Civil, Environmental and Sustainable Engineering, Arizona State University, 243 pp.).
Anderson, V.J., Hodgkinson, K.C., 1997. Grass-mediated capture of resource flows and the maintenance of banded mulga in a semi- arid woodland. Aust. J. Bot. 45, 331–342.
Anderson, C.A., Vivoni, E.R., 2016. Impact of land surface states within the flux footprint on daytime land- atmosphere coupling in two semiarid ecosystems of the Southwestern U.S. Water Resour. Res. 52, 4785–4800.
Barbier, N., Couteron, P., Lejoly, J., Deblauwe, V., Lejeune, O., 2006. Self-organized vegetation patterning as a fingerprint of climate and human impact on semi-arid ecosystems. J. Ecol. 94 (3), 537–547.
Bautista, S., Mayor, A.G., Bourakhouadar, J., Bellot, J., 2007. Plant spatial pattern predicts hillslope runoff and erosion in a semiarid Mediterranean landscape. Ecosystems 10 (6), 987–998.
Berg, S.S., Dunkerley, D.L., 2004. Patterned Mulga near Alice Springs, central Australia, and the potential threat of firewood collection on this vegetation community. J. Arid Environ. 59 (2), 313–350.
Bhark, E.W., Small, E.E., 2003. Association between plant canopies and the spatial patterns of infiltration in shrubland and grassland of the Chihuahuan Desert, New Mexico. Ecosystems 6 (2), 185–196.
Boer, M., Puigdefábregas, J., 2005. Effects of spatially structured vegetation patterns on hillslope erosion in a semiarid Mediterranean environment: a simulation study. Earth Surf. Process. Landf. 30, 149–167.
Calvo-cases, A., Boix-Fayos, C., Imeson, A.C., 2003. Runoff generation, sediment movement and soil behavior on calcareous (limestone) slopes of some Mediterranean environments in southeast Spain. Geomorphology 50, 269–291.
Cammeraat, L.H., Imeson, A.C., 1999. The evolution and significance of soil–vegetation patterns following land abandonment and fire in Spain. Catena 37 (1–2), 107–127.
Cavanaugh, M.L., Kurc, S.A., Scott, R.L., 2011. Evapotranspiration partitioning in semiarid shrubland ecosystems: a two-site evaluation of soil moisture control on transpiration. Ecohydrology 4, 671–681.
Cerdà, A., 1997. The effect of patchy distribution of Stipa tenacissima Lon runoff and erosion. J. Arid Environ. 36 (1), 37–51.
Cerdan, O., Le Bissonnais, Y., Govers, G., Lecomte, V., van Oost, K., Couturier, A., King, C., Dubreuil, N., 2004. Scale effect on runoff from experimental plots to catchments in agricultural areas in Normandy. J. Hydrol. 299 (1–2), 4–14.
Chen, L., Sela, S., Svoray, T., Assouline, S., 2013. The role of soil-surface sealing, microtopography, and vegetation patches in rainfall-runoff processes in semiarid areas. Water Resour. Res. 49, 5585–5599.
Couteron, P., Lejeune, O., 2001. Periodic spotted patterns in semi-arid vegetation explained by a propagation-inhibition model. J. Ecol. 89 (4), 616–628.
Deblauwe, V., Couteron, P., Bogaert, J., Barbier, N., 2012. Determinants and dynamics of banded vegetation pattern migration in arid climates. Ecol. Monogr. 82 (1), 3–21.
Dunkerley, D.L., 2002. Infiltration rates and soil moisture in a groved mulga community near Alice Springs, arid central Australia: evidence for complex internal rainwater redistribution in a runoff–runon landscape. J. Arid Environ. 51 (2), 199–219.
Dunne, T., Zhang, W., Aubry, B.F., 1991. Effects of rainfall, vegetation and microtopography on infiltration and runoff. Water Resour. Res. 27, 2271–2285.
Ferrante, D., Oliva, G.E., Fernández, R.J., 2014. Soil water dynamics, root systems, and plant responses in a semiarid grassland of Southern Patagonia. J. Arid Environ. 104, 52–58.
Fuentes, D., Smanis, A., Valdecantos, A., 2016. Recreating sink areas on semiarid degraded slopes by restoration. Land Degrad. Dev. 28 (3), 1005–1015.
Galle, S., Ehrmann, M., Peugeot, C., 1999. Water balance in a banded vegetation pattern. A case study of tiger bush in western Niger. Catena 37 (1–2), 197–216.
Garcia-Estringana, P., Alonso-Blázquez, N., Alegre, J., 2010. Water storage capacity, stemflow and water funnelling in Mediterranean shrubs. J. Hydrol. 389, 363–372.
Geris, J., Tetzlaff, D., McDonnell, J., Soulsby, C., 2017. Spatial and temporal patterns of soil water storage and vegetation water use in humid northern catchments. Sci. Total Environ. 595, 486–493.
Hao, H.M., Lu, R., Liu, Y., Fang, N.F., Wu, G.L., Shi, Z.H., 2016. Effects of shrub patch size succession on plant diversity and soil water content in the water-wind erosion crisscross region on the Loess Plateau. Catena 144, 177–183.
Howes, D., Abrahams, A.D., 2003. Modeling runoff and runon in a desert shrubland ecosystem, Jornada Basin, New Mexico. Geomorphology 53, 45–73.
Jin, C.X., Romkens, M.J.M., Griffioen, F., 2000. Estimating Manning's roughness coefficient for shallow overland flow in non- submerged vegetative filter strips. Trans. ASAE 43 (6), 1459–1466.
Johnson, P.O., Neyman, J., 1936. Tests of certain linear hypothesis and their application to some educational problems. Stat. Res. Mem. 1, 57–93.

Katra, I., Blumberg, D.G., Lavee, H., Sarah, P., 2007. Topsoil moisture patterns on arid hillsides - micro-scale mapping by thermal infrared images. J. Hydrol. 334 (3–4), 359–367.
King, W.E., Hawley, J.W., 1975. Geology and ground-water resources of the Las Cruces area, New Mexico. In: Seager, W.R., Clemons, R.E., Callender, J.F. (Eds.), New Mexico Geological Society 26th Annual Fall Field Conference Guidebook, pp. 195–204 (376 pp.).
Laliberte, A.S., Rango, A., 2011. Image processing and classification procedures for analysis of sub-decimeter imagery acquired with an unmanned aircraft over arid rangelands. GIScience Remote Sens. 48 (1), 4–23.
Lavee, H., Imeson, A.C., Pariente, S., 1998. The impact of climate change on geomorphology and desertification along a Mediterranean-arid transect. Land Degrad. Dev. 9, 407–422.
Lozano-Parra, J., Schnabel, S., Ceballos-Barbancho, A., 2015. The role of vegetation covers on soil wetting processes at rainfall event scale in scattered tree woodland of Mediterranean climate. J. Hydrol. 529, 951–961.
Ludwig, J.A., Wilcox, B.P., Breshears, D.D., Tongway, D.J., Imeson, A.C., 2005. Vegetation patches and runoff-erosion as interacting ecohydrological processes in semi-arid landscape. Ecology 86 (2), 288–297.
Magliano, P.N., Breshears, D.D., Fernández, R.J., Jobbágy, E.G., 2015. Rainfall intensity switches ecohydrological runoff/runon redistribution patterns in dryland vegetation patches. Ecol. Appl. 25 (8), 2094–2100.
Marques, M.J., Bienes, R., Jiménez, L., Pérez-Rodríguez, R., 2007. Effect of vegetal cover on runoff and soil erosion under light intensity events. Rainfall simulation over USLE plots. Sci. Total Environ. 378 (1–2), 161–165.
Mekonnen, M., Keesstra, S.D., Ritsema, C.J., Stroosnijder, L., Baartman, J.E.M., 2016. Sediment trapping with indigenous grass species showing differences in plant traits in Northwest Ethiopia. Catena 147, 755–763.
Merino-Martín, L., Breshears, D.D., Moreno-de Las Heras, M., Villegas, J.C., Pérez-Domingo, S., Espigares, T., Nicolaue, J.N., 2011. Ecohydrological source-sink interrelationships between vegetation patches and soil hydrological properties along a disturbance gradient reveal a restoration threshold. Restor. Ecol. 20 (3), 360–368.
Merino-Martín, L., Moreno-de Las Heras, M., Espigares, T., Nicolau, J.M., 2015. Overland flow directs soil moisture and ecosystem processes at patch scale in Mediterranean restored hillslopes. Catena 133, 71–84.
Moreno-de Las Heras, M., Saco, P.M., Willgoose, G.R., Tongway, D.J., 2012. Variations in hydrological connectivity of Australian semiarid landscapes indicate abrupt changes in rainfall-use efficiency of vegetation. J. Geophys. Res. 117 (G3), 1–15.
Newman, B.D., Campbell, A.R., Wilcox, B.P., 1997. Tracer-based studies of soil water movement in semi-arid forests of New Mexico. J. Hydrol. 251–270 (3), 196.
Okin, G.S., Moreno-de Las Heras, M., Saco, P.M., Throop, H.L., Vivoni, E.R., Parsons, A.J., Wainwright, J., Peters, D.C., 2015. Connectivity in dryland landscapes: shifting concepts of spatial interactions. Front. Ecol. Environ. 13 (1), 20–27.
Pan, J., Bai, Z., Cao, Y., Zhou, W., Wang, J., 2017. Influence of soil physical properties and vegetation coverage at different slope aspects in a reclaimed dump. Environ. Sci. Pollut. Res. 24 (30), 23953–23965.
Parsons, A.J., Brazier, R.E., Wainwright, J., Powell, D.M., 2006. Scale relationships in hillslope runoff and erosion. Earth Surf. Process. Landf. 31 (11), 1384–1393.
Paschalis, A., Katul, G.G., Simone, F., Manoli, G., Molnar, P., 2016. Matching ecohydrological processes and scales of banded vegetation patterns in semiarid catchments. Water Resour. Res. 52, 333–1352.
Pierini, N.P., Vivoni, E.R., Robles-Morua, A., Scott, R.L., Nearing, M.A., 2014. Using observations and a distributed hydrologic model to explore runoff thresholds linked with mesquite encroachment in the Sonoran Desert. Water Resour. Res. 50, 8191–8215.
Puigdefábregas, J., 2005. The role of vegetation patterns in structuring runoff and sediment fluxes in drylands. Earth Surf. Process. Landf. 147, 133–147.
Puigdefábregas, J., Sánchez, G., 1996. Geomorphological implications of vegetation patchiness on semi-arid slopes. In: Anderson, M.G., Brooks, S.M. (Eds.), Advances in Hillslope Processes vol. 2. JohnWiley & Sons Ltd., London, pp. 1027–1060.
Puigdefábregas, J., Sole, A., Gutierrez, L., Barrio, G., Boer, M., 1999. Scales and processes of water and sediment redistribution in drylands: results from the Rambla Honda field site in Southeast Spain. Earth-Sci. Rev. 48, 39–70.
Reid, K.D., Wilcox, B.P., Breshears, D.D., MacDonald, L., 1999. Runoff and erosion in a Piñon–Juniper woodland: influence of vegetation patches. Soil Sci. Soc. Am. J. 63 (6), 1869.
Renard, K.G., 1988. Water resources of small impoundments in dry regions. In: Thames, J.L., Ziebell, C.D. (Eds.), Small Water Impoundments in Semiarid Regions. University of New Mexico Press, Albuquerque, NM, USA.
Rietkerk, M., Boerlijst, M.C., van Langevelde, F., HilleRisLambers, R., van de Koppel, J., Kumar, L., Prins, H.H.T., de Roos, A.M., 2002. Self-organization of vegetation in arid ecosystems. Am. Nat. 160, 524–530.
Rossi, M.J., Ares, J.O., 2016. Overland flow from plant patches: coupled effects of preferential infiltration, surface roughness and depression storage at the semiarid Patagonian Monte. J. Hydrol. 533, 603–614.
Rossi, M.J., Ares, J.O., 2017. Water fluxes between inter-patches and vegetated mounds in flat semiarid landscapes. J. Hydrol. 546, 219–229.
Rostagno, C.M., del Valle, H.F., 1988. Mounds associated with shrubs in aridic soils of northeastern Patagonia: characteristics and probable genesis. Catena 15, 347–359.
Saco, P.M., Moreno-de Las Heras, M., 2013. Ecogeomorphic coevolution of semiarid hillslopes: emergence of banded and striped vegetation patterns through interaction of biotic and abiotic processes. Water Resour. Res. 49 (1), 115–126.
Saco, P.M., Willgoose, G.R., Hancock, G.R., 2007. Eco-geomorphology of banded vegetation patterns in arid and semi-arid regions. Hydrol. Earth Syst. Sci. 11 (6), 1717–1730.
Schreiner-McGraw, A.P., Vivoni, E.R., 2017. Percolation in arid piedmont watersheds: observations from an instrument network and linkages to historical conditions. Ecosphere 8 (11). https://doi.org/10.1001/ecs2.2000.
Schreiner-McGraw, A.P., Vivoni, E.R., Mascaro, G., Franz, T.E., 2016. Closing the water balance with cosmic-ray soil moisture measurements and assessing their spatial variability within two semiarid watersheds. Hydrol. Earth Syst. Sci. 12 (6), 5343–5388.
Scoging, H.M., Parsons, A.J., Abrahams, A.D., 1992. Application of a dynamic overland-flow hydraulic model to a semi-arid hill-slope, Walnut Gulch, Arizona. In: Parsons, A.J., Abrahams, A.D. (Eds.), Overland Flow Hydraulics and Erosion Mechanics. UCL Press, London, UK, pp. 105–145.
Stoof, C.R., Vervoort, R.W., Iwema, J., van den Elsen, E., Ferreira, A.J.D., Ritsema, C.J., 2012. Hydrological response of a small catchment burned by experimental fire. Hydrol. Earth Syst. Sci. 16, 267–285.
Templeton, R.C., Vivoni, E.R., Mendez-Barroso, L.A., Pierini, N.A., Anderson, C.A., Rango, A., Laliberte, A.S., Scott, R.L., 2014. High-resolution characterization of a semiarid watershed: implications on evapotranspiration estimates. J. Hydrol. 509, 306–319.
Thompson, S.E., Katul, G., Konings, A., Ridolfi, L., 2011. Unsteady overland flow on flat surfaces induced by spatial permeability contrasts. Adv. Water Resour. 34 (8), 1049–1058.
Tongway, D.J., Valentin, C., Seghieri, J., 2001. Banded vegetation patterning in arid and semiarid environments: ecological processes and consequences for management. Ecological Studies vol. 149. Springer-Verlag, New York, USA.
Traff, D.C., Niemann, J.D., Middlekauff, S.A., Lehman, B.M., 2014. Effects of woody vegetation on shallow soil moisture at a semiarid montane catchment. Ecohydrology 947, 935–947.
Valentin, C., D'Herbes, J.M., Poesen, J., 1999. Soil and water components of banded vegetation patterns. Catena 37 (1–2), 1–24.
van de Giesen, N.C., Stomph, T.J., de Ridder, N., 2000. Scale effects of Hortonian overland flow and rainfall-runoff dynamics in a West African catena landscape. Hydrol. Process. 14 (1), 165–175.
Venables, W.N., Ripley, B.D., 2002. Modern Applied Statistics With S. Springer Science & Media Inc., New York, NY, US.
Wainwright, J., Parsons, A.J., Abrahams, A.D., 2000. Plot-scale studies of vegetation, overland flow and erosion interactions: case studies from Arizona and New Mexico. Hydrol. Process. 14, 2921–2943.
Wegmann, M., Leutner, B.F., Metz, M., Neteler, M., Dech, S., Rocchini, D., 2017. r.pi: a grass gis package for semi-automatic spatial pattern analysis of remotely sensed land cover data. Methods Ecol. Evol. 1–9 (May).
Wilcox, B.P., 2003. Runoff from rangelands: the role of shrubs. In: McGinty, A., Hanselka, C.W., Ueckert, D.N., Hamilton, W., Lee, M. (Eds.), Shrub Management. Texas A&M University, College Station, Texas.
Wilcox, B.P., Breshears, D.D., Allen, C.D., 2003. Ecohydrology of a resource-conserving semi-arid woodland: effects of scale and disturbance. Ecol. Monogr. 73, 223–239.
Wu, G.L., Wang, D., Liu, Y., Hao, H.M., Fang, N.F., Shi, Z.H., 2016. Mosaic-pattern vegetation formation and dynamics driven by the water-wind crisscross erosion. J. Hydrol. 538, 355–362.
Yu, M., Gao, Q., Epstein, H.E., Zhang, X., 2008. An ecohydrological analysis for optimal use of redistributed water among vegetation patches. Ecol. Appl. 18 (7), 1679–1688.